Advanced Considerations in the Implementation of Security-Constrained Optimal Power Flow (SCOPF) for Electricity Markets

Santiago Grijalva
santiago@powerworld.com
PowerWorld Corporation, IL, USA

Abstract
This paper describes how the SCOPF provides signals agents need to interact in electricity markets and some of the advanced features needed for its implementation. These include: sensitivity analysis, AC and DC options for both power flow and contingency analysis solutions, approximated limits including reactive power flows, unenforceable constraint management, modeling of load response as a control through curtailment contracts, determination of reactive power LMP's, modeling of nonlinear limits such as voltage stability and dynamic ATC through nomograms, variable area transfer pricing, and spatio-temporal analysis.

1. Introduction

The primary goal of deregulated electricity markets is the production of price signals that reveal economic information and produce incentives for investment and efficiency. In pursuing these goals, several electricity market models have been proposed and implemented in different countries and regions. The locational marginal price (LMP) model continues to consolidate itself as the market mechanism to generate signals required by electricity market agents. Most of the current competitive electricity markets operate their systems based on the locational model or are moving towards it [1,2].

LMPs provide signals with embedded information that reflect the most relevant aspects of system generation costs and transmission congestion, and thus communicate signals for markets. The locational marginal pricing market model has the advantage of being compatible with the physics of the power grid, something not trivial to achieve. In addition, the locational pricing model is compatible with other market structures such as bilateral transactions and interconnections. In an electricity market that combines long term bilateral transactions with a location spot market, the bilateral prices should converge to real-time locational marginal prices (LMP). Bilateral transaction should accordingly be priced based on LMP forecasting.

The SCOPF algorithm [2-6] has established itself as the tool required to generate LMPs that include information about general supply and demand equilibrium, marginal losses, normal operation congestion and post-contingency congestion. Since all these aspects are relevant for the economic and secure operation of the market, the LMPs should contain no less information than the one provided by the SCOPF. This paper describes how the SCOPF function captures the information agents need to interact in the market and some of the advanced features required for its implementation in realistic large-scale electricity markets.

2. Electricity Market Studies

Electricity market studies are developed in order to determine whether a particular market meets its goals and whether specific problems in design, operation, monitoring, and regulation are likely to arise. Successful electricity markets are characterized by generation adequacy and investment, system security, and efficiency. Generation adequacy deals with the market mechanisms that ensure that capacity and reserve are available in the long term (investments). System security deals with the signals provided by the market to expand the transmission grid, so the system can withstand load growth and operate secure at all times. Efficiency is related to the prices converging to equilibrium close to generation marginal costs.

These are all broad aspects that require detailed, time-dependent analysis of how buyers and sellers interact in the locational market. This interaction though takes place "through" the grid, and thus detailed modeling of the network configuration and its limitations is required. Central to the analysis of electricity markets it is the determination of LMPs, which facilitate developing among others, the following types of studies.

a) Market Design:
   - Price equilibrium analysis
   - Market volatility
   - Investment
   - Hydro marginal pricing
b) Market Operations:
   - Congestion management and re-dispatch
   - Congestion revenue
   - Interconnection pricing
   - Bilateral Transfer Pricing
c) Market Monitoring and Regulation
   - Profit maximization analysis
   - Market power and strategic gaming
   - Price forecasting
   - Price sensitivity analysis
   - Price cap effects

3. LMPs as a Sub-product of SCOPF

The LMP is the marginal cost of serving (an infinitesimal amount of) additional active power load at a certain node in the system. The LMP can be obtained through diverse algorithms of increasing levels of complexity:

a) The prices reflect energy cost and are consistent with the optimal dispatch of the next megawatt-hour. This corresponds to the classical economic dispatch (ED) without losses. It assumes that all the buyers and sellers are connected to a single point or, what is the same, that the power grid is lossless, that individual elements have infinite capacity and that any transfer has unlimited available transfer capability (ATC).
b) Besides including the cost of energy, the prices can include marginal active power transmission losses. This would correspond to the economic dispatch with losses. This assumes that the power grid has infinite capacity and ATC, and thus no congestion.
c) Beside energy and marginal losses, the prices reflect the enforcement of normal operation constraints such as transmission element thermal limits. If a constraint is binding, it is said that there is congestion and the LMP has a congestion component. These prices can be determined using a standard optimal power flow (OPF) algorithm
d) Beyond energy, marginal losses, and normal operation congestion, the prices reflect the enforcement of security limits under events, such as single contingencies. Prices may therefore have a contingency congestion component. A SCOPF algorithm is required to find these security-constrained locational marginal prices (SCLMP).

Most advanced markets currently operating are based on security-constrained dispatch and consequently utilize real-time or quasi-real-time SCOPF software applications. Efficient implementation of security-related information requires using sensitivities, which are more naturally obtained and implemented in a linear-programming (LP) OPF [3], as opposed to in a nonlinear OPF. LP OPF is usually related to active power optimization rather than reactive power optimization and hence market applications use implementations based on LP. In addition to solving problems that involve contingencies, the LP-based SCOPF can efficiently detect and handle infeasible cases, something that becomes critical when modeling system contingencies. We start describing the SCOPF formulation.

The SCOPF problem requires the solution of a set of non-linear equations, which can be expressed as:

$$\begin{aligned} &\text{Minimize:} && F(\mathbf{x},\mathbf{u}) \\ &\text{Subject to:} && \mathbf{g}(\mathbf{u},\mathbf{x}) = \mathbf{0} \\ & && \mathbf{h}(\mathbf{u},\mathbf{x}) \le \mathbf{0} \\ & && \mathbf{v}(\mathbf{u},\mathbf{x}) \le \mathbf{0} \end{aligned} \qquad (1)$$

where $\mathbf{x}$ is the vector of dependent variables and $\mathbf{u}$ is the vector of system controls. Examples of control variables are the real power generator output, phase shifter angle, net interchange, load MW dispatch associated to load curtailment block contracts, and DC transmission line flow settings.

In (1) $F(\mathbf{x},\mathbf{u})$ is the objective function, which can be either:

- Active power operating cost minimization
- Active power losses minimization
- Minimum control shift
- Minimum number of controls rescheduled

$\mathbf{g}(\mathbf{x},\mathbf{u})$ is a set of nonlinear equality constraints that correspond to the power flow mismatch equations. $\mathbf{h}(\mathbf{x},\mathbf{u})$ is a set of inequality constraints that correspond to normal operating limits, and $\mathbf{v}(\mathbf{x},\mathbf{u})$ is a set of inequality constraints related to contingency constraints.

The nonlinear optimization problem in (1) is solved as a succession of linear approximations:

$$\begin{aligned} &\text{Minimize:} \quad F(\mathbf{x}^{(k)},\mathbf{u}^{(k)}) \\ &\text{Subject to:} \quad \mathbf{g}'(\mathbf{x}^{(k)},\mathbf{u}^{(k)}) = \mathbf{0} \\ &\qquad\qquad\quad \mathbf{h}'(\mathbf{x}^{(k)},\mathbf{u}^{(k)}) \le \mathbf{0} \\ &\qquad\qquad\quad \mathbf{v}'(\mathbf{x}^{(k)},\mathbf{u}^{(k)}) \le \mathbf{0} \end{aligned} \tag{2}$$

Where $\mathbf{x}^{(k)}$ and $\mathbf{u}^{(k)}$ are the values of $\mathbf{x}$ and $\mathbf{u}$ at the k^{th} approximation, which are obtained as:

$$\begin{aligned} \mathbf{x}^{(k)} &= \mathbf{x}^{(k-1)} + \Delta\mathbf{x}^{(k-1)} \\ \mathbf{u}^{(k)} &= \mathbf{u}^{(k-1)} + \Delta\mathbf{u}^{(k-1)} \end{aligned} \tag{3}$$

$\mathbf{g}', \mathbf{h}'$ and $\mathbf{v}'$ are the linear approximations of the original nonlinear constraints. The sequential solution technique yields the sequential linear programming SCOPF, which is implemented as follows:

while $\Delta\mathbf{x} > \varepsilon$ **do**
  solve the AC power flow
  solve the contingency analysis
  determine sensitivities.
  solve the SCOPF problem defined in (2)
  update the control variables
end

4. Sensitivity Calculations

One of the most remarkable properties of a highly-nonlinear system such as an electric power system is the well-behaved approximate linear relation between active power injections and active power flow. If an injection of active power takes place somewhere in the system and this generation is balanced by a sink somewhere else, the resulting changes in flows in all the transmission lines will be proportional to the transfer. LP formulation of the SCOPF uses linear sensitivities to determine the rows of the LP-tableau and how controls will affect the objective function. In this section we summarize the computation of linear sensitivities with respect to a transfer.

We model a power transfer as $p\mathbf{T}$, were p is the transfer size in megawatt or per unit, and $\mathbf{T}$ is a vector of buying and selling participation factors: $\mathbf{T} = \mathbf{T}_S + \mathbf{T}_B$, such that:

$$\begin{aligned} &\mathbf{T} = \begin{bmatrix} 0 & PF_x^{sell} & 0 & PF_y^{sell} & 0 & PF_j^{buy} & 0 & PF_k^{buy} \end{bmatrix}^T \\ &\sum_{h=1}^{n} PF^{sell} = 1 \quad \text{and} \quad \sum_{i=1}^{n} PF^{buy} = -1 \end{aligned} \tag{4}$$

$\mathbf{T}$ may correspond to a transfer from a single bus to the slack, representing in this case the movement of a generation active power control. At p=0, the system is in the base case, presumably a pre-optimized, pre-contingency condition. The voltage and angle sensitivities with respect to the size of the transfer are then:

$$\begin{bmatrix} \Delta\boldsymbol{\theta} \\ \Delta\mathbf{V} \end{bmatrix} = [\mathbf{J}]^{-1} \begin{bmatrix} p\mathbf{T} \\ \mathbf{0} \end{bmatrix}; \tag{5}$$

We do not consider in this paper the problem of loss allocation schemes, which assign the system losses either to the seller or the buyer and thus determine or assume a value of κ in $\mathbf{T} = \mathbf{T}_S + \kappa\mathbf{T}_B$. From (5) it is clear that:

$$\begin{bmatrix} \dfrac{\partial\boldsymbol{\theta}}{\partial p} \\ \dfrac{\partial\mathbf{V}}{\partial p} \end{bmatrix} = [\mathbf{J}]^{-1} \begin{bmatrix} \mathbf{T} \\ 0 \end{bmatrix} \tag{6}$$

With these expressions, we can calculate the required sensitivities for the SCOPF. First, the active power power transfer distribution factor (PTDF) gives the change in line flow with respect to the active power injection (change in generator MW output):

$$\begin{aligned} \rho_{km,\mathbf{T}} &= \frac{\partial P_{km}}{\partial p} \\ &= \left(\frac{\partial P_{km}}{\partial \theta_k}\frac{\partial \theta_k}{\partial p} + \frac{\partial P_{km}}{\partial \theta_m}\frac{\partial \theta_m}{\partial p} + \frac{\partial P_{km}}{\partial V_k}\frac{\partial V_k}{\partial p} + \frac{\partial P_{km}}{\partial V_m}\frac{\partial V_m}{\partial p} \right)\mathbf{T} \end{aligned} \tag{7}$$

Let us define a vector of active power line flows for existing lines km, which may include flows at both ends of the transmission lines:

$$\boldsymbol{\varphi}^P = \begin{bmatrix} P_{12} & P_{21} & \cdots & P_{km} & P_{mk} & \cdots & P_{n-1,n} \end{bmatrix}^T \tag{8}$$

The sensitivity of this vector with respect to the transfer is a vector of PTDFs:

$$\begin{aligned} \boldsymbol{\rho}_{\mathbf{T}} &= \frac{\partial\boldsymbol{\varphi}^P}{\partial p} = \frac{\partial\boldsymbol{\varphi}^P}{\partial\boldsymbol{\theta}}\frac{\partial\boldsymbol{\theta}}{\partial p} + \frac{\partial\boldsymbol{\varphi}^P}{\partial\mathbf{V}}\frac{\partial\mathbf{V}}{\partial p} \\ &= \begin{bmatrix} \dfrac{\partial\boldsymbol{\varphi}^P}{\partial\boldsymbol{\theta}} & \dfrac{\partial\boldsymbol{\varphi}^P}{\partial\mathbf{V}} \end{bmatrix} \begin{bmatrix} \partial\boldsymbol{\theta}/\partial p \\ \partial\mathbf{V}/\partial p \end{bmatrix} \\ &= \begin{bmatrix} \dfrac{\partial\boldsymbol{\varphi}^P}{\partial\boldsymbol{\theta}} & \dfrac{\partial\boldsymbol{\varphi}^P}{\partial\mathbf{V}} \end{bmatrix} [\mathbf{J}]^{-1} \begin{bmatrix} \mathbf{T} \\ \mathbf{0} \end{bmatrix} \end{aligned} \tag{9}$$

Now let us describe the computation of line outage sensitivities. Using single index notation, consider two lines *l* and *k*. The line outage distribution factor (LODF) is the fraction of the pre-contingency flow on line *k* that will show up on line *l* after line *k* is opened.

$$\lambda_{l,k} = \frac{\Delta P_{l,k}}{P_k} \tag{10}$$

The linear impact of this line outage can be determined by modeling the outage as a transfer between the terminals of the line. Let us denote by P_k^f the size of the transfer such that the flow in the line is zero, i.e., it is equivalent to opening the line. The value of P_k^f is unknown. The change in the flow on line *l* after the transfer is equal to $\Delta P_{l,k} = \rho_l \times P_k^f$. The flow on line *k* after the transfer is equal to $P_k^f = P_k^0 + \rho_k \times P_k^f$. Hence, $P_k^f = P_k / (1 - \rho_k)$. Thus the LODF can be written as:

$$\lambda_{l,k} = \frac{\rho_l \times P_k^f}{P_k} = \frac{\rho_l}{P_k} \times \left(\frac{P_k}{1 - \rho_k} \right) = \frac{\rho_l}{1 - \rho_k} \tag{11}$$

Note that the LODF becomes a simple relation of PTDF's. Since contingencies may include not only line openings, but also line closures, we require computing the line closure distribution factors (LCDF). This is the fraction of the pre-closure flow on line *k* that will show up on line *l* after closing line *k*:

$$\gamma_{l,k} = \frac{\Delta P_{l,k}}{P_k^f} \tag{12}$$

The linear impact of a line closure is also determined by modeling the closure as a transfer between the terminals of the line. A transfer of size $-P_k^f$ can be set between buses as a linear equivalent to opening the transmission line. Let us assume that we now this value. The post-closure flow on line *l* is equal to $\Delta P_{l,k} = -\rho_l \times P_k^f$. Thus we can write:

$$\gamma_{l,k} = \frac{\Delta P_{l,k}}{P_k^f} = \frac{-\rho_l \times P_k^f}{P_k^f} = -\rho_l \tag{13}$$

Thus the LCDF is exactly equal to the negative of the PTDF for a transfer between the terminals of the line.

5. DC SCOPF

Within the SCOPF solution, the solution of the power flow and the contingency analysis may be either AC or DC. In the AC approach, each contingency is implemented at a time and the full AC power flow solution is obtained. In the DC contingency analysis, linear sensitivities are computed to model element outages and to determine post-contingency flows using these linear sensitivities. These sensitivities are also utilized in the linearized constrained equations $\mathbf{g}'$,$\mathbf{h}'$ and $\mathbf{v}'$ and can be utilized to make the SCOPF the fastest algorithm. A critical feature of the SCOPF should be therefore AC and DC options. While the AC solution will be exact, major computational savings can be obtained when doing DC power flow or DC contingency analysis.

We now describe the determination of the sensitivities needed for DC contingency analysis and DC SCOPF. When using DC power flow equations we are interested only on the angle sensitivities. Equation (5) above becomes [7]:

$$\left[\frac{\partial \boldsymbol{\theta}}{\partial p} \right] = \left[\mathbf{B}' \right]^{-1} \mathbf{T} \tag{14}$$

The distribution factors are calculated modifying equation (7) as:

$$\begin{aligned} \rho_{km,\mathbf{T}} &\simeq \left(\frac{\partial P_{km}}{\partial \theta_k} \frac{\partial \theta_k}{\partial P} + \frac{\partial P_{km}}{\partial \theta_m} \frac{\partial \theta_m}{\partial P} \right) \mathbf{T} \\ &\simeq -b_{jk} \left(\frac{\partial \theta_k}{\partial P} - \frac{\partial \theta_m}{\partial P} \right) \mathbf{T} \end{aligned} \tag{15}$$

and the vector of distribution factors in (9) therefore becomes:

$$\boldsymbol{\rho}_{\mathbf{T}} = \frac{\partial \boldsymbol{\varphi}^P}{\partial \boldsymbol{\theta}} \left[\mathbf{B} \right]^{-1} \mathbf{T} \tag{16}$$

6. Approximation of Reactive Flows

One of the assumptions of DC methods is that reactive power is zero. This assumption is sometimes convenient because besides not needing to compute any reactive power flows or voltage quantities, it allows equating MVA and MW transmission line limits. Under this assumption, a 150MVA line can carry 150MW of active power. However, this assumption may become inaccurate in stressed lines carrying some significant amount of reactive power.

Furthermore, it may result in some lines that would be binding in the AC solution, not being binding in the DC solution, with the consequent differences in the LMP due to the inaccurate congestion component.

Let us denote by $S_{km}^{\max}$ the thermal limit of line *km* expressed as pu of MVA. We also assume that the flows in both ends of the line are equal: $P_{jk}=P_{kj}$. There are three options in DC SCOPF regarding reactive power flows and limits:

a) Assume $Q_{jk} = 0$, then $P_{km}^{\max} = S_{km}^{\max}$
b) Assume that the reactive power is constant. Then $P_{km}^{\max} = \sqrt{\left(S_{km}^{\max}\right)^2 - \left(Q_{km}^{0}\right)^2}$.
c) Assume that the voltages at the ends of the line are constant. In this case it turns out that a Mvar- corrected limit can be derived.

Consider the active and reactive power flows of a line from bus *j* to bus *k*:

$$\begin{aligned} P_{jk} &= V_j^2 G_{jk} - V_j V_k Y_{jk} \cos(\theta_j - \theta_k + \alpha_{jk}) \\ &= P_{jk\odot} - S_{jk\odot} \cos\gamma_{jk} \end{aligned} \quad (17)$$

$$\begin{aligned} Q_{jk} &= -V_j^2 B_{jj} + V_j^2 B_{jk} - V_j V_k Y_{jk} \sin(\theta_j - \theta_k + \alpha_{jk}) \\ &= Q_{jk\odot} - S_{jk\odot} \sin\gamma_{jk} \end{aligned} \quad (18)$$

Taking the square of both sides and adding, we obtain the equation of the complex flow in the P_{jk}-Q_{jk} plane. This is called the transmission line operating circle [8]:

$$(P_{jk} - P_{jk\odot})^2 + (Q_{jk} - Q_{jk\odot})^2 = (S_{jk\odot})^2 \quad (19)$$

This is the circle followed by the complex flow of line *jk*. This circle has center at $(P_{jk\odot}, Q_{jk\odot})$ and radius equal to $S_{jk\odot} = V_j V_k Y_{jk}$. Since the voltages at the line ends are assumed to be constant, the terms with subscript $\odot$ denote a constant parameter.

Equation (19) provides a fast method to check limits including reactive power either in power flow or contingency analysis. Once the DC solution is obtained and for instance the post-contingency flow in the lie is known to be P_{jk}, we plug this value in (19) to obtain Q_{jk} as a function of P_{jk}:

$$Q_{jk}(P_{jk}) = Q_{jk\odot} + \sqrt{(S_{jk\odot})^2 - (P_{jk} - P_{jk\odot})^2} \quad (20)$$

The resulting value of reactive power $S_{jk} = \sqrt{P_{jk}^2 + Q_{jk}^2}$ can be compared with $S_{jk}^{\max}$ to identify a thermal violation.

The inverse problem of determining how much active power can be increased in the line to reach the limit is more difficult. We need to determine the intersection of the operating circle and a limiting circle given by the constraint that $P_{jk}^2 + Q_{jk}^2 = (S_{jk}^{\max})^2$. This is illustrated in Figure 1.

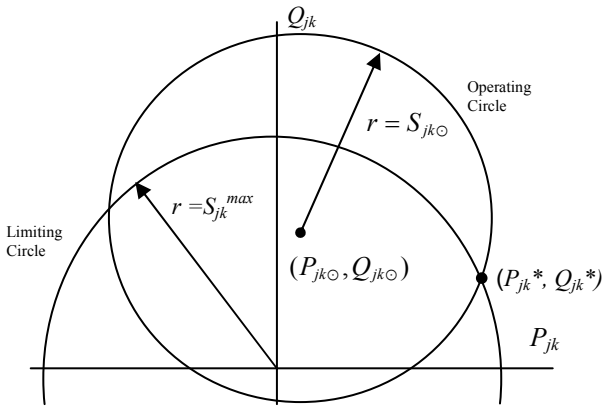

Figure 1: Operating and Limiting Circles

In order to compute P_{jk}^* and Q_{jk}^* the following system of equations must be solved:

$$\begin{aligned} (P_{jk} - P_{jk\odot})^2 + (Q_{jk} - Q_{jk\odot})^2 &= S_{jk\odot}^{\ 2} \\ P_{jk}^{\ 2} + Q_{jk}^{\ 2} &= (S_{jk}^{\max})^2 \end{aligned} \quad (21)$$

Expanding the first equation and subtracting the second one we obtain:

$$Q_{jk} = \frac{1}{2Q_{jk\odot}}\left(-2P_{jk}P_{jk\odot} + (S_{jk}^{\max})^2 - M^2\right) \quad (22)$$

where $M^2 = S_{jk\odot}^{\ 2} - P_{jk\odot}^{\ 2} - Q_{jk\odot}^{\ 2}$. Substituting back into the limiting circle equation the following quadratic expression in P_{jk}^* is obtained:

$$\begin{aligned} &(P_{jk\odot}^{\ 2} + Q_{jk\odot}^{\ 2})P_{jk}^{*2} - P_{jk\odot}\left((S_{jk}^{\max})^2 - M^2\right)P_{jk}^* + \\ &+\tfrac{1}{4}\left((S_{jk}^{\max})^2 - M^2\right)^2 - Q_{jk\odot}^{\ 2}(S_{jk}^{\max})^2 = 0 \end{aligned} \quad (23)$$

Defining the corresponding constant coefficients:

$$a = (P_{jk\odot}{}^2 + Q_{jk\odot}{}^2); \quad b = -P_{jk\odot}\left((S_{jk}{}^{\max})^2 - M^2\right)$$
$$c = \tfrac{1}{4}\left((S_{jk}{}^{\max})^2 - M^2\right)^2 - Q_{jk\odot}{}^2 (S_{jk}{}^{\max})^2 \quad (24)$$

the solution for the maximum complex flow is obtained as:

$$P_{jk}{}^{*} = \frac{-b \pm \sqrt{b^2 - 4ac}}{2a}; \quad Q_{jk}{}^{*} = \sqrt{(S_{jk}{}^{\max})^2 - P_{jk}{}^{*2}} \quad (25)$$

The sign in the previous equation is chosen to be positive if the PTDF of line *j-k* is positive and negative otherwise. In order to incorporate the maximum active flow P_{jk}^{*} in the DC SCOPF the only change required is to replace $S_{jk}^{\max}$ by P_{jk}^{*}. P_{jk}^{*} represents a better approximation to the actual maximum active line flow due to the transfer by considering the reactive power flow component.

7. Inclusion of Nonlinear Limits

One of the challenges in SCOPF is the modeling of limits that vary depending on the system conditions. Examples are flowgate flows and generator operating limits. In the LP-SCOPF, these can be modeled by using nomograms, i.e., linear descriptions of how a linear limit changes as a function of other variables. For instance consider a system with two flowgates A and B, with limits L_A= 400MW and L_B = 300MW. Let us assume that these flowgates cannot be loaded to their limits simultaneously due to a voltage stability limit: the sum of the two flowgate flows is constrained to less than 500MW.

The implementation of the limit in the SCOPF consists in just adding this equation to the inequality constraints. However, some equations may be more involved. In this case, there are two options: automatically generate a piece-wise linear function as a set of multiple equations, or let the user graphically define the nonlinear constraint and thus the line segments. The constraint equations, illustrated in Figure 2 for the example would be:

$$\begin{aligned} &\phi_A - 400 \le 0 \\ &\phi_B - 300 \le 0 \\ &\phi_A + \phi_B - 500 \le 0 \\ &\mathbf{f}(\phi_A, \phi_B) \le 0 \end{aligned} \quad (26)$$

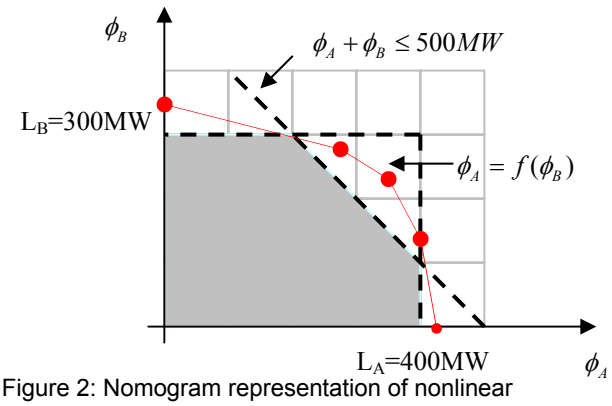

Figure 2: Nomogram representation of nonlinear constraints.

8. Variable Price Transfer

The optimization outcome of a control area depends on its internal resources as well as on external conditions of the grid, such as area interchanges. In assessing the potential effect of external resources, it is important to be able to model variable-price transfers between control areas. There are two main types of transactions that can be implemented in the SCOPF:

a) Auto-priced transfers: When both areas are on OPF control, then the transaction is auto-priced. There is no need to specify a price for the transaction. The amount and price of the transfer is optimally determined by the algorithm. This functionality allows one to easily combine areas, with the added flexibility of being able to put limits on the amount of power transferred and placing a transmission charge on the transfer.
b) Specified Variable-Cost Transfer: When a transaction includes only one area on OPF control then the user needs to enter a cost for the transaction. The values should be entered for buying and selling and they should be monotonically increasing. Piece-wise linear cost curves are specified for both the Export and Import transactions, which can have a maximum and minimum value, and a transaction charge.

If only one transaction area is on OPF control, then the optimal amount of the transfer is implemented by the OPF. If multiple areas are on OPF, then the transfer is auto-priced. As an example to illustrate these concepts consider the seven bus case shown in Figure 3. All areas are dispatched in OPF, and the area interchange is zero.

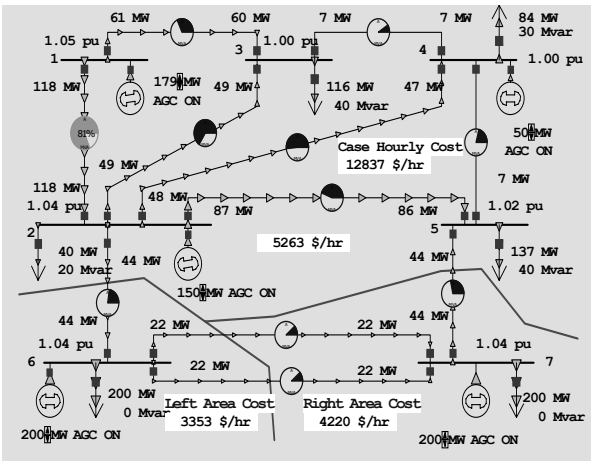

Figure 3: OPF Solution without Transactions

Let us now consider a transfer from Area Right to Left. The LP-OPF determines -79.8 MW as the optimal transfer. The resulting operating state is shown in Figure 4. The net interchanges of areas Right and Left are now +79.8 and -79.8, respectively. The system operating cost has decreased from 12,837 $/hr to 12,518 $/hr. This effectively models the simultaneous optimization with the area transaction as a control.

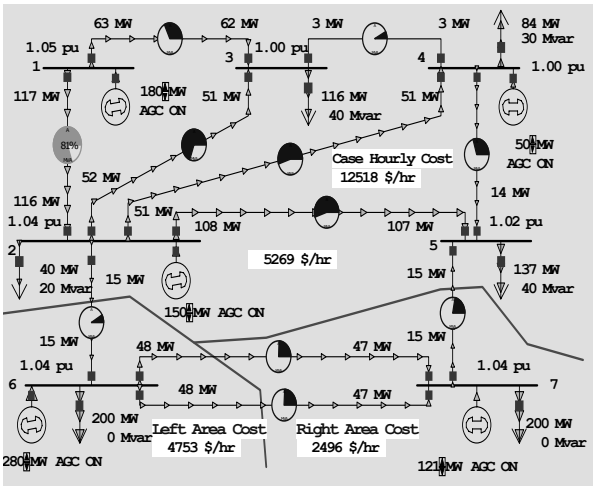

Figure 4: A Transaction from Area Right to Left

Let us go back to the state obtained after solving the case with all areas in OPF and no transactions (Figure 3). We optimize area Right by dispatching areas Top and Left under participation factor control. A variable price transaction from Right to Left is defined. The optimization identifies an optimal import of 5 MW into area Right. The system operating cost is now 12,812 $/MWhr, i.e., 15 $/MWhr less than in the case without transactions.

9. Modeling of Load Curtailment Contracts

Modeling price-response for demand in a power system is implemented as the price-response for generation. For generation, as the price at a generator bus increases, the desired output of that generator will *increase*. For demand, as the price at a load bus increases, the desired use of that load will *decrease*. A load represents an injection of power which is opposite in sign to a generator. Because generator and load injections have opposite sign and their responses are also opposite in sign, mathematically these two models are identical in the formulation of an optimal power flow algorithm.

The following example shows the effect of demand response in a system. Consider a 3-bus system, with 3 loads, 3 generators, and 3 transmission lines divided in 2 control areas. All the generators have economic data, and are set available for AGC. The benefit linear curves for loads at buses 2 and 3 are shown in Figures 5.

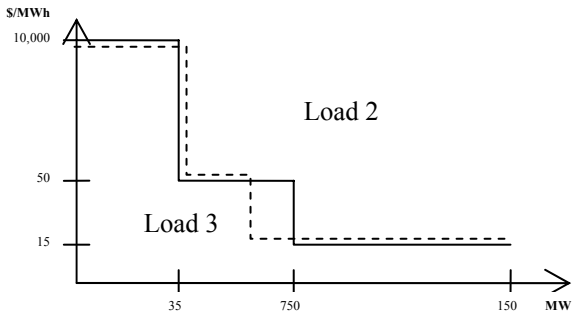

Figure 5: Load benefit curves for load 2 and 3

Figure 6 shows the case being dispatched with OPF by control area. Because all the loads are Off AGC, they are not included in the OPF process. As it can be observed, the transmission line from bus 1 to 3 is loaded at its maximum capacity.

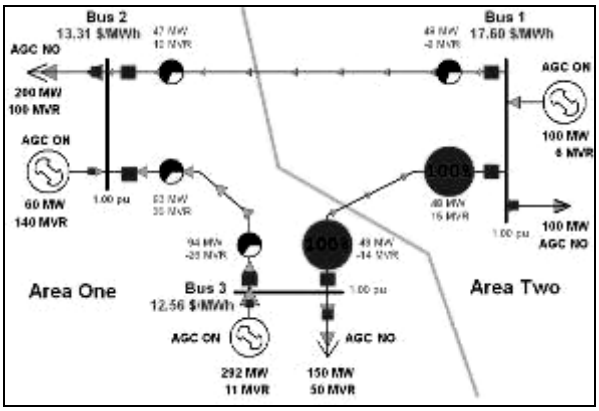

Figure 6: Base case dispatched with OPF

Figure 7 shows the case when generator at bus 3 is open. The OPF dispatch can not enforce the constraint on the line from bus 1 to 3. Because the OPF has encountered an unenforceable transmission line constraint, the marginal prices determined only indicate the buses where potential load-shedding would be needed. The absolute numbers for marginal prices are not directly useable, because we have not actually met all the constraints posed to the OPF. In this example, the load at Bus 3 would need to be involuntarily curtailed.

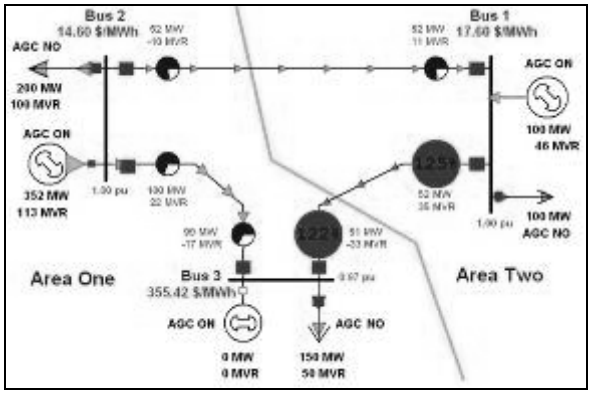

Figure 7: OPF dispatch after opening Gen at bus 3

When loads are set to AGC allowing for demand price-response and they are included in the OPF solution, load at bus 3 can step back from 150 MW to 112 MW, so that the marginal cost at bus 3 meets the demand curve specified in Figure 5, which shows a price of 15.0 $/MWh at bus 3. The line constraint from bus 1 to 3 can be now enforced. Figure 8 shows the resulting case.

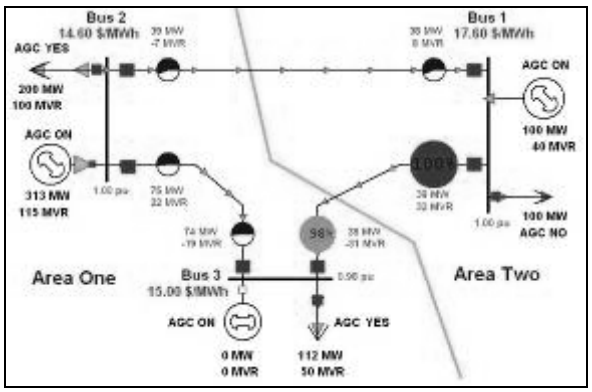

Figure 8: OPF dispatch with load demand response

10. Unenforceable Constraints

During the linear programming solution, the OPF may detect conditions where the system does not have enough controls to enforce a constraint. This means that the LP problem is infeasible. In order to reach a valid solution, the OPF relaxes the unenforceable constraint and prices this condition. Unenforceable constraints are often the result of modeling problems, such as incorrect line limits or insufficient contingency RAS modeling. Unenforceable constraints that indicate the actual inability of the system to comply with a certain level of security need to be priced to provide signals of the need to design system expansion or to use load response.

Consider the case whose initial condition is shown in Figure 9. The generators in this case have hard minimum and maximum limits. Area interchange constraints are also enforced. The total load in area top is 400MW, with scheduled imports of 50MW. Without contingencies, all the constraints are enforceable and the thermal limit of line 1 to 2 has become a binding constraint.

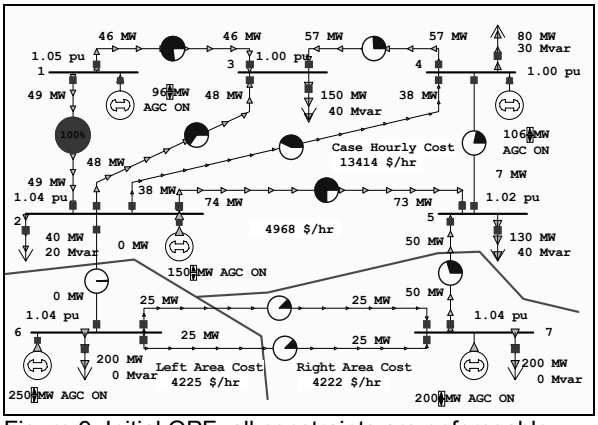

Figure 9: Initial OPF: all constraints are enforceable

Let us simulate the case of an unenforceable constraint. If line 5 to 7 is opened, Line 2 to 5 becomes overloaded at 5% and the OPF cannot enforce this constraint, as shown in Figure 10.

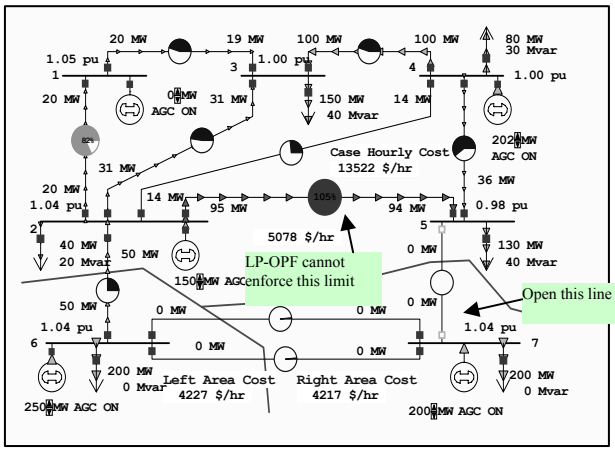

Figure 10: OPF with One Unenforceable Constraint

Line 2-5 is unenforceable because in the post-contingency condition, lines 2 to 5 and 4 to 5 serve the 130MW and 40Mvar load at bus 5. Generator 1 and generator 2 are both at their low output limit (0MW and 150MW, respectively). Generator 4 has to produce the necessary power to balance the active power load plus losses plus interchange of area Top. Generators 1 and 2 cannot generate less and Generator 4 cannot generate more. Consequently, there are no controls in the system that can be moved to mitigate the overload at line 2 to 5.

Note that if the MVA limit of line 2 to 5 were about 105MVA instead of 100MVA, then the constraint would be enforceable. The generators did move attempting to enforce the constraint changing the LMPs in the system. This brings us to the problem of unenforceable constraint pricing.

The price associated with enforcing a constraint is equal to the price of moving generator controls to make the constraint binding. When the constraint is unenforceable, the LP problem is infeasible and the unenforceable constraint needs to be relaxed to achieve a solution. In the previous example if about 5 MW load the load at bus 5 are shed, then the constraint could become enforceable. Thus the price of the unenforceable constraint should be comparable to the cost of shedding that amount of load. Since this cost may be significant, we can expect that unenforceable constraints have an important effect on the LMP prices.

It is customary to assign a constant $/hr cost to every unenforceable line or interface constraint. This cost does not depend on the severity of the overload and is usually equal set at 1000 $/hr, although it can be higher. Note that a price of 0 $/hr will result in the line and interface limits not being enforced by the OPF. The cost assigned to the unenforceable constraint will be distributed to the bus LMP based on the sensitivities of each bus injection to the flow of the unenforceable line or interface. In the previous example, an increase on the load at bus 5 will worsen the overload of line 2 to 5. The LMP of bus 5 would be higher because it is at the receiving end of the constraint.

Another option is to assign to the unenforceable constraint a variable cost based on the percentage overload of the element limit. This cost is modeled as a piecewise linear marginal cost in $/MWhr. If applied to lines and interfaces, limit costs can be modeled within AC and DC modes of the OPF and SCOPF.

When interpreting the causes of unenforceable constraints several aspects need to be analyzed. The OPF approach must attempt to model the system as close as possible to how it is actually operated. The analyst should always ask himself how the system would be operated in reality.

Line Limits: The behavior of unenforceable constraints, even with variable pricing is highly sensitive to the value of the limits. A realistic selection of the limits used in the optimization problem is crucial to obtaining consistent LMP results. Utilities use different thermal ratings for normal operation, contingency, and emergency operation. The correct use of different sets of limits in OPF and SCOPF will affect the correct identification of unenforceable constraints and the final LMPs.

Contingency Set: The SCOPF considers a set of plausible contingencies, which model a certain level of network security. The contingency set determines LMPs that provide weak or strong security signals. Since the desired level of security is given by operating and market policies, the selection of the contingency set is ultimately a policy decision. In regional studies, the contingency list should include at least the highest voltage elements and those that have been compiled in a historical database. A more restrictive analysis should include *N*-1 and common mode contingencies. The set of critical contingencies recommended by operation engineers should be included in the operations planning environment. Markets and RTOs usually have rules about which contingencies should be modeled in planning studies or market operations.

Remedial Action Schemes (RAS): The contingency definition in SCOPF studies should consider operating schemes that are to be implemented in case of severe contingencies or emergencies RAS may include load shedding and other operating actions designed to mitigate the post-contingency overloads. Not modeling RAS may have a significant impact in the LMP outcome as it does in security analysis.

Load Response: The response of load should be included within the controls of the OPF algorithm. Interruptible contracts based on price, as well as demand response are modeled by specifying load benefit curves. Responsive loads will

contribute significantly when unenforceable constraints need to be eliminated.

Variable Limit Pricing: The variable cost of unenforceable constraints is somehow arbitrary. Unenforceable constraints that are due to modeling problems need to be corrected before a final pricing scheme is implemented. When unenforceable constraints result from actual limitations of the system there are two alternatives: a) Remove the element form the monitored set and treat that element outside the OPF; and b) Price the infeasibility condition of that element. In the later case, it is reasonable to assume that the cost will depend on the overload levels, e.g., different levels of line upgrade or load shedding would have different cost.

A value of 200 $/MWhr can be used as the minimum cost at the 100% break point. This value is usually higher than the cost of energy delivered and comparable to congestion LMPs. It is also comparable to price caps that have been implemented in different markets to avoid price volatility. A contingency overload of 50% (150% flow) is considered severe. A price above 1000 $/Hr is set for this level.

11. Reactive Power LMPs

SCOPF should have the capability of computing reactive power LMPs, which are defined as the change in total operating cost that results from serving an additional Mvar of load at a certain bus. Calculating these values is a post-solution activity so it has no impact on the solution itself.

Since the system operating cost is determined by the cost of producing active power, reactive power has an indirect effect on the cost: an increase in the reactive power load served will change the flows in the system and the active power losses. This change in losses needs to be met by active power generation.

Consider the three bus system show in Figure 11, which has three identical lines with parameters r = 0.03 pu and x = 0.1 pu. The line limits are 100MVA. The incremental cost of generators 1, 2 and 3 are 10, 12, and 20 $/MWh, respectively. For an initial load of 100 MW and 30Mvar at bus 3, the active power LMP at bus 3 is equal to 10.45 $/MWh and the reactive power LMP is equal to 0.12 $/Mvarh.

As expected, since reactive power LMPs are related to losses, they are in general small compared to active power LMPs. If the system is lossless and has no congestion, then the reactive power LMPs would be equal to zero. On the other hand, if the system has congestion, then the reactive power LMPs may become significant, since the sensitivity of reactive power injection to the MVA flow of a (binding) line may not be small.

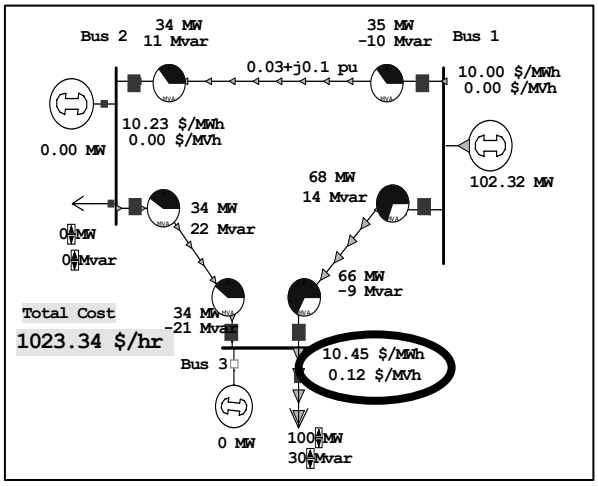

Figure 11: 3-bus system with no congestion.

Consider the same system with a load of 180 MW and 30 Mvar and include marginal losses in the calculation. Then the active power LMP is 15.11 $/MWh and the reactive power LMP is equal to 1.00 $/Mvarh, as shown in Figure 12.

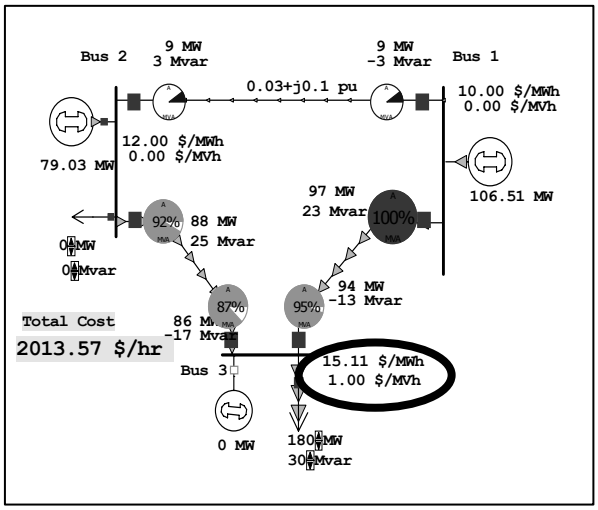

Figure 12: 3-bus system with congestion.

In the same manner, reactive power LMPs may be significant in the case of unenforceable constraints. For this three bus case a 1,000 $/MWh has been set as penalty for line unenforceable constraints. If the load at bus 3 increases to 200 MW and 30 MVar, then

generators 1 and 2 cannot supply the power to the load without overloading at least one line. If a LP-OPF solution is attempted, then the OPF will identify the MVA limit of line 1 to 3 as an unenforceable constraint and assign the mentioned penalty cost. The resulting active and reactive power LMPs at bus 3 become 1,129.53 $/MWh and 288.93 $/Mvarh, respectively.

The reactive power LMPs are available only in the AC OPF and SCOPF simulations. However, they can also be obtained in the AC OPF with DC Contingency Analysis solution. Note that the inclusion of marginal losses in the LMP computation will affect the values of the reactive power LMP. The reactive power LMPs are valid only at PQ buses. At a PV bus and at the slack bus the cost of reactive power is zero since it can immediately be supplied by the generator.

12. Spatio-Temporal SCOPF Analysis

Visualization is a key feature within large-scale power system analysis and electricity market simulation. Spatial visualization methods allow the analyst to process thousands of data points at a time capturing spatial relations that cannot be discovered in a tabular manner.

Figure 13 shows spatial contouring visualization of the Tennessee Valley Authority (TVA) case for the summer 2000. Darker colors indicate lower market prices while higher color regions indicate high market prices. By analyzing the contouring one can determine the causes of price gradients, such as congestion and market power. This is critical not only for actual operations, but also for electricity market design, regulation and monitoring.

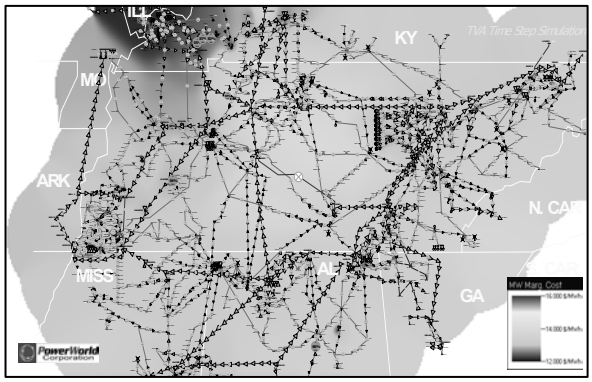

Figure 13: TVA system price contouring

Another important feature of OPF and SCOPF is the possibility to run multiple hourly cases in a single simulation instance in order to compare results and to explore the evolution of power system quantities across time, in particular, nodal prices. This is achieved through flexible data structures that allow loading arrays of varying hourly and scheduled data into the SCOPF engine. Figure 14 shows the temporal behavior of TVA's total demand during August 2000, hour by hour. The lower part of the Figure shows how the MW output of two large generators change in time when the system is dispatched by the SCOPF.

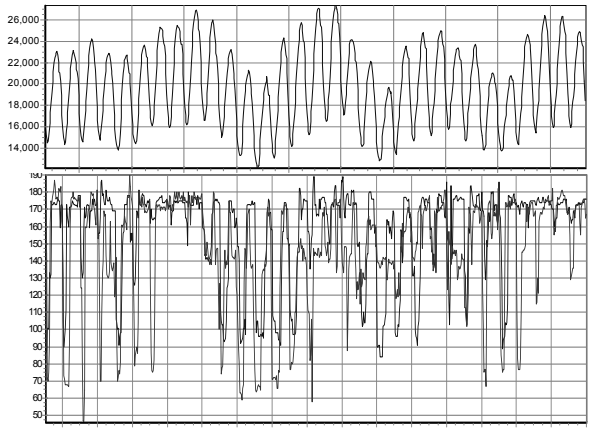

Figure 14: Hourly Results of SCOPF

In addition, temporal SCOPF functions allow determining system congestion and congestion revenues for the different participants in the market. This is achieved by running for each hour two simulations: an unconstrained OPF and a full SCOPF. The difference between the LMPs obtained with these two solution methods corresponds to the cost of congestion.

13. Conclusions

SCOPF based LMPs are able to capture the physical aspects of the power grid and provide prices that include the effect of energy costs, marginal losses, normal operation constraints and contingency limitations. These prices represent signals to agents that help markets achieve adequacy, security and efficiency.

Sequential linear programming SCOPF has consolidated itself as a core algorithm that drives electricity markets based on locational marginal prices. Besides being a large-scale complex problem, the SCOPF problem requires that software applications be equipped with advanced flexible features able to meet the requirements of modern power system: sensitivity analysis, AC and DC options for power flow and contingency solutions, Mvar limit correction, variable-price

transfer, inclusion of nonlinear limits through nomograms, management of unenforceable constraints, and spatio-temporal analysis tools.

These advanced features have resulted in successful SCOPF software implementations in systems that run large-scale electricity markets.

14. References

[1] Ott, A.L., "Experience with PJM Market Operation, System Design, and Implementation", IEEE Transactions on Power Systems, Vol. 18, No. 2, May 2003, pp: 528- 534.

[2] Huang, J.; Yalla, P.; Yong, T., "New Real Time Market Applications At The California Independent System Operator (CAISO)", IEEE PES Power Systems Conference and Exposition, 10-13 Oct. 2004, Vol. 3, pp: 1228 -1233.

[3] Alsac, O.; Bright, J.; Prais, M.; Stott, B., "Further Developments in LP-based Optimal Power Flow", IEEE Transactions on Power Systems, Vol 5. No. 3, Aug. 1990, pp: 697- 711.

[4] Momoh, J.A.; Koessler, R.J.; Bond, M.S.; Stott, B.; Sun, D.; Papalexopoulos, A.; Ristanovic, P., "Challenges to Optimal Power Flow", IEEE Transactions on Power Systems, Vol. 12, No. 1, Feb. 1997, pp: 444- 455.

[5] Jabr, R.A.; Coonick, A.H.; Cory, B.J., "A Homogeneous Linear Programming Algorithm for the Security Constrained Economic Dispatch Problem", IEEE Transactions on Power Systems, Vol. 15, No. 3, Aug. 2000, pp: 930-936.

[6] Shahidehpour, M.; Tinney, F.; Yong Fu, "Impact Of Security On Power Systems Operation, Proceedings of the IEEE, Vol. 93, No. 11, Nov. 2005 , pp: 2013-2025.

[7] Sauer, P.W.; Reinhard, K.E.; Overbye, T.J., "Extended Factors for Linear Contingency Analysis. Proceedings of the 34th Annual Hawaii International Conference on System Sciences, Jan. 2001, pp: 697-703.

[8] Grijalva, S.; Sauer, P.W.; Weber, J.D., "Enhancement Of Linear ATC Calculations By The Incorporation Of Reactive Power Flows", IEEE Transactions on Power Systems, Vol. 18, No. 2, May 2003, pp: 619-624.

[9] Overbye, T.J.; Xu Cheng; Yan Sun, "A Comparison of the AC and DC power flow models for LMP Calculations", Proceedings of the 37th Annual Hawaii International Conference on System Sciences, Jan, 2004.

[10] Weber, J.D.; Overbye, T.J.; Sauer, P.W.; DeMarco, C.L., "A Simulation Based Approach to Pricing Reactive Power", Proceedings of the Thirty-First Hawaii International Conference on System Sciences, 6-9 Jan. 1998, Vol 3, pp: 96 -103.

[11] Weber, J.D.; Overbye, T.J.; DeMarco, C.L., "Inclusion Of Price Dependent Load Models In The Optimal Power Flow", Proceedings of the Thirty-First Hawaii International Conference on System Sciences, 6-9 Jan. 1998, Vol. 3, pp:62 -70.

[12] Overbye, T.J., "Estimating The Actual Cost Of Transmission System Congestion", Proceedings of the 36th Annual Hawaii International Conference on System Sciences, Jan. 2003.

Biography

Santiago Grijalva obtained the Electrical Engineer degree from EPN-Ecuador in 1994, the M.S. Certificate in Information Systems from ESPE-Ecuador in 1997, and the M.S. and Ph.D. Degrees in Electrical Engineering from the University of Illinois at Urbana-Champaign in 1999 and 2002, respectively. He completed the Post-Doctoral program in Power and Energy Systems at the University of Illinois in 2004. From 1995 to 1997, he was with the Ecuadorian National Center for Energy Control (CENACE) as EMS engineer and Head of the Software Department. Since 2001 he develops advanced power system applications for PowerWorld Corporation. He has been a consultant for major government agencies and utilities across the US. During 2005 and 2006 he was an invited professor at EPN where he taught graduate courses on advanced power system analysis and power system economics. His areas of interest are real-time systems, power system computational algorithms, and electricity markets.